



Universiteit  
Leiden  
The Netherlands

## Glycoform analysis of intact erythropoietin by MALDI FT-ICR mass spectrometry

Lippold, S.; Thavarajah, R.; Reusch, D.; Wuhrer, M.; Nicolardi, S.

### Citation

Lippold, S., Thavarajah, R., Reusch, D., Wuhrer, M., & Nicolardi, S. (2021). Glycoform analysis of intact erythropoietin by MALDI FT-ICR mass spectrometry. *Analytica Chimica Acta*, 1185. doi:10.1016/j.aca.2021.339084

Version: Publisher's Version

License: [Creative Commons CC BY 4.0 license](https://creativecommons.org/licenses/by/4.0/)

Downloaded from: <https://hdl.handle.net/1887/3246775>

**Note:** To cite this publication please use the final published version (if applicable).



## Glycoform analysis of intact erythropoietin by MALDI FT-ICR mass spectrometry

Steffen Lippold<sup>a,1,\*</sup>, Raashina Thavarajah<sup>a,1</sup>, Dietmar Reusch<sup>b,2</sup>, Manfred Wuhrer<sup>a,1</sup>, Simone Nicolardi<sup>a,1,\*</sup>

<sup>a</sup> Center for Proteomics and Metabolomics, Leiden University Medical Center, Leiden, the Netherlands

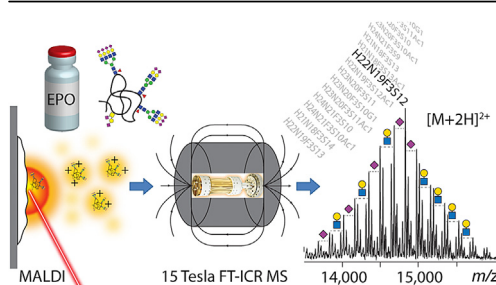
<sup>b</sup> Pharma Technical Development Penzberg, Roche Diagnostics GmbH, Penzberg, Germany



### HIGHLIGHTS

- Fast glycoform-resolved profiling of highly sialylated intact EPO was achieved using MALDI FT-ICR MS.
- The loss of sialic acid residues was minimized by using DHAP as a MALDI matrix.
- Straightforward data analysis was performed on doubly charged ions, solely, without the need for any charge deconvolution.
- The method showed potential for high-throughput applications and the analysis of other glycoproteins up to 40 kDa.

### GRAPHICAL ABSTRACT



### ARTICLE INFO

#### Article history:

Received 6 July 2021

Received in revised form

13 September 2021

Accepted 19 September 2021

Available online 21 September 2021

#### Keywords:

MALDI FT-ICR MS

Intact protein

Sialic acid

Erythropoietin

Glycosylation

Biopharmaceuticals

### ABSTRACT

Recombinant human erythropoietin (EPO) is a complex therapeutic glycoprotein with three *N*- and one *O*-glycosylation sites. Glycosylation of EPO influences its safety and efficacy and is defined as a critical quality attribute. Thus, analytical methods for profiling EPO glycosylation are highly demanded. Owing to the complexity of the intact protein, information about EPO glycosylation is commonly derived from released glycan and glycopeptide analysis using mass spectrometry (MS). Alternatively, comprehensive insights into the glycoform heterogeneity of intact EPO are obtained using ESI MS-based methods with or without upfront separation of EPO glycoforms. MALDI MS, typically performed with TOF mass analyzers, has been also used for the analysis of intact EPO but, due to the poor glycoform resolution, has only provided limited glycoform information. Here, we present a MALDI FT-ICR MS method for the glycoform profiling of intact EPO with improved glycoform resolution and without loss of sialic acid residues commonly observed in MALDI analysis. Three EPO variants were characterized in-depth and up to 199 glycoform compositions were assigned from the evaluation of doubly-charged ions, without any deconvolution of the mass spectra. Key glycosylation features such as sialylation, acetylation, and *N*-acetylactosamine repeats were determined and found to agree with previously reported data obtained from orthogonal analyses. The developed method allowed for a fast and straightforward data acquisition and evaluation and can be potentially used for the high-throughput comparison of EPO samples throughout its manufacturing process.

© 2021 The Author(s). Published by Elsevier B.V. This is an open access article under the CC BY license (<http://creativecommons.org/licenses/by/4.0/>).

\* Corresponding authors. Leiden University Medical Center, Center for Proteomics and Metabolomics, Albinusdreef 2, 2333 ZA Leiden, the Netherlands.

E-mail addresses: [s.lippold@lumc.nl](mailto:s.lippold@lumc.nl) (S. Lippold), [s.nicolardi@lumc.nl](mailto:s.nicolardi@lumc.nl) (S. Nicolardi).

<sup>1</sup> Steffen Lippold – Center for Proteomics and Metabolomics, Leiden University Medical Center, 2333 ZA Leiden, The Netherlands; [orcid.org/0000-0002-1032-5808](https://orcid.org/0000-0002-1032-5808).

<sup>2</sup> Dietmar Reusch – Pharma Technical Development, Roche Diagnostics GmbH, 82377 Penzberg, Germany.

## 1. Introduction

Recombinant human erythropoietin (EPO) is a complex glycoprotein and a very successful biopharmaceutical [1–3]. The protein backbone is about 18,000 Da with additional glycosylation that extends the molecular mass up to about 32,000 Da. Four glycosylation sites (Asn24, Asn38, Asn83, and Ser126) and a high diversity of structural glycosylation features (varying levels of antennae, *N*-acetylglucosamine (LacNAc) repeats, sialylation, phosphorylation, sulfation, acetylation) have been described [4]. Since these features affect the safety and efficacy profile of EPO, glycosylation – defined as a critical quality attribute (CQA) of EPO – must be characterized to ensure the quality of the biopharmaceutical [5].

The in-depth glycosylation analysis of complex glycoproteins, such as EPO, is typically performed by a combination of different mass spectrometry (MS)-based methods [6,7]. In fact, since the very first reports on the structure and function of EPO, MS has been widely used to study its glycosylation. The integration of information, obtained from multiple analysis levels, is needed for a comprehensive characterization of EPO glycosylation (Fig. 1).

The analysis of enzymatically released glycans has provided detailed information of the *N*-glycosylation of EPO [4,8–11], while the analysis of glycopeptides has allowed for a site-specific determination of the glycan compositions [5,12–17]. At the intact protein level, MS provides unique information on the combinatorial presence of different glycan moieties on its four glycosylation sites [8,18–22]. However, such an analysis, that leads to very complex mass spectra, is challenged by the high glycoform heterogeneity. This problem has been often mitigated by combining powerful separation techniques with sensitive MS methods [19,23–26]. For example, the use of anion exchange chromatography (AEX) and Fourier transform ion cyclotron resonance (FT-ICR) MS has recently allowed for the assignment of 357 proteoforms to an EPO reference standard (EPO RS) [27]. Such an in-depth analysis requires long measurement times and tedious data processing, therefore, more direct strategies have also been developed. For example, in a recent report by Caval and co-workers, intact glycoengineered variants of EPO were analyzed by native ESI MS on a modified Orbitrap MS

system without any upfront separation [28]. The assignment of up to 236 EPO glycoforms allowed for comprehensive glycoform profiling of EPO [21]. Direct analysis methods were demonstrated to be very powerful for fast glycoform profiling and similarity assessment. Of note, the high heterogeneity of EPO limits the applicability of top-down MS/MS strategies therefore the analysis of intact EPO proteoforms, as well as other glycoproteins of similar complexity, must be always complemented by other structural analyses such as bottom-up MS.

Intact protein analysis of EPO has also been performed by MALDI MS however, this type of analysis has only provided limited information since the different EPO glycoforms are typically not resolved in time-of-flight (TOF) MS that is the most commonly used type of MALDI MS [29–32]. Furthermore, MALDI analysis of sialylated glycans and glycoconjugates is often affected by the loss of sialic acid residues that occurs during or post ionization. Compared to ESI MS, MALDI MS methods offer the advantage of a faster acquisition, the absence of carryover, a more stable ion source performance, and a more straightforward data interpretation. Therefore, a MALDI MS method for the analysis of intact EPO, with glycoform resolution and without loss of sialic acid residues, would be of great benefit.

In this study, we developed a MALDI FT-ICR MS method for the analysis of intact EPO glycoforms. Three EPO variants, namely EPO RS, EPO RP+ and EPO RP- were analyzed using 2,5-dihydroxyacetophenone as a MALDI matrix to minimize the loss of sialic acid residues. Robust and detailed glycosylation profiles were obtained directly from the evaluation of doubly charged EPO glycoforms, without any deconvolution of the mass spectra. The precise assignment of glycoform compositions allowed for the evaluation of key glycosylation features of EPO such as sialylation, acetylation, and LacNAc repeats. The developed method allowed for a straightforward comparison of EPO variants and can be potentially used throughout the manufacturing process for example for clonal selection, batch-to-batch comparison, and biosimilars evaluation.

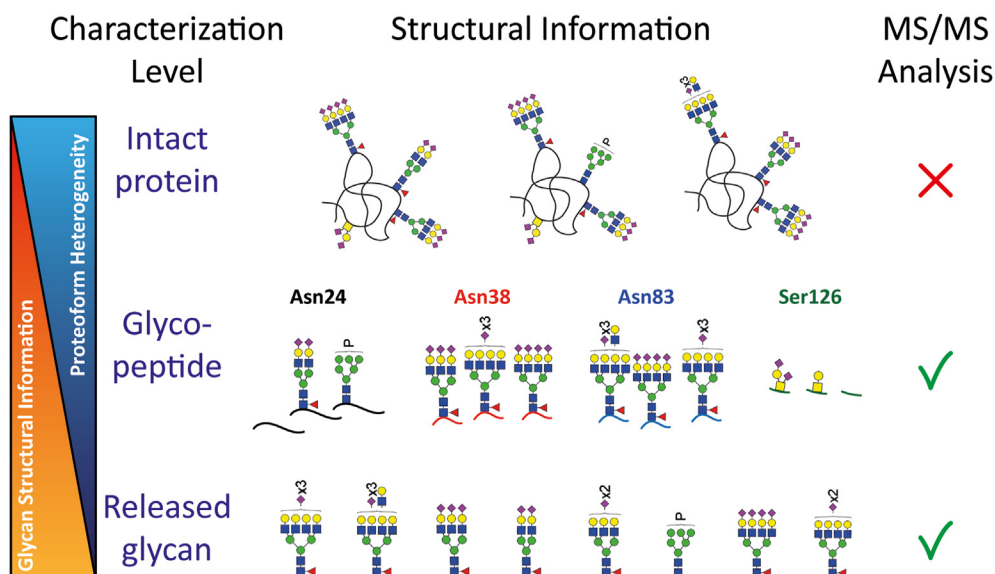


Fig. 1. Scheme of multi-level characterization of EPO using MS-based methods.

## 2. Experimental section

### 2.1. Chemicals and samples

All chemicals used in this study had at least analytical grade quality and were, if not otherwise stated, purchased from Sigma Aldrich (Steinheim, Germany). EPO RS, EPO RP+, and EPO RP- were produced in Chinese hamster ovary (CHO) cells and were kindly provided by Roche Diagnostics (Penzberg, Germany). EPO RP+ and EPO RP- were obtained from EPO after fractionation by reversed-phase HPLC, as described elsewhere [5]. All EPO materials were previously studied by several methods and reference data was used for comparison [5,16,27]. Precisely, the very same samples used in this studies were previously characterized by bottom-up MS at a glycopeptide level and the obtained MS/MS spectra are available at <https://doi.org/10.25345/C54998> [16]. For MALDI MS analysis, 2,5-dihydroxyacetophenone (DHAP, saturated) mixed in a ratio 8:2 with diammonium hydrogen citrate (DAHC, 20 mg/mL), in acetonitrile (ACN):water (50:50%, v/v), was used as MALDI matrix. 4-Chloro- $\alpha$ -cyanocinnamic acid (CICCA) was prepared at 10 mg/mL in ACN:water (70:30%, v/v) while, saturated sinapic acid (SA) and saturated  $\alpha$ -cyano-4-hydroxycinnamic acid (CHCA) were prepared in ACN:water:trifluoroacetic acid (30:69.9:0.1%, v/v/v). For external calibration of the MS system, 10 mM *trans*-2-[3-(4-*tert*-butylphenyl)-2-methyl-2-popenylidene]malononitrile (DCTB) in acetone was used as MALDI matrix to analyze cesium iodide cluster ions  $[(Cs)_n + Cs]^+$ .

### 2.2. Desialylation

Enzymatic desialylation of EPO RS was performed using SialEXO® (Genovis). 50  $\mu$ g of EPO were digested with 50 units SialEXO (40 units/ $\mu$ L) in 20 mM tris(hydroxymethyl)aminomethane buffer, pH 6.8 at 37 °C for 4 h.

### 2.3. Sample clean-up

The EPO samples were subjected to solid-phase extraction (SPE) by C4 ZipTip® tips (Merck Millipore). The SPE-tip was washed three times with 10  $\mu$ L of ACN:water:formic acid (FA) (50:49.9:0.1%, v/v/v). Then, the SPE-tip was conditioned, three times, with 10  $\mu$ L of 0.1% FA in water. Prior to loading, 10  $\mu$ g of the sample were diluted in 10  $\mu$ L with 0.1% FA in water. Upon sample loading (20 times), an additional washing step (five times methanol:water:FA (5:94.9:0.1%, v/v/v)) was applied and the sample was eluted in 10  $\mu$ L of ACN:water:FA (50:49.9:0.1%, v/v/v).

### 2.4. MALDI spotting

0.5  $\mu$ L of the EPO samples were spotted onto a polished steel target MALDI plate (Bruker Daltonics) and 0.5  $\mu$ L of DHAP matrix were added. For external calibration of the MS system, 0.5  $\mu$ L CsI<sub>3</sub> (50 mM in water) was spotted together with 0.5  $\mu$ L of DCTB matrix [33]. The spots were allowed to dry at room temperature.

### 2.5. MALDI FT-ICR MS

A 15 T solariX XR FT-ICR mass spectrometer (Bruker Daltonics) with a CombiSource and a ParaCell was used in the study. The mass spectrometer was operated using ftmsControl software (Bruker Daltonics). MALDI experiments were performed with a Smartbeam-II Laser System (Bruker Daltonics) at a frequency of 500 Hz and 200 laser shots. The “selective accumulation” mode was used to sum 200 high-quality spectra. The data were acquired in positive-ion mode in the  $m/z$ -range 2022–35,000 with 64,000 data

points (*i.e.* transient time 0.2884 s). The total measurement time was approximately 5 min. The MS instrument was externally calibrated using  $[(Cs)_n + Cs]^+$  ion clusters (Fig. S1). All samples were measured in triplicates. For EPO RS, two additional measurements were performed on two days for interday analysis. Additionally, linear positive-mode MALDI TOF MS measurements were performed on a rapifleX mass spectrometer (Bruker Daltonics).

### 2.6. Data analysis

Mass spectra were visualized and inspected in DataAnalysis 5.0 (Bruker Daltonics). mMass was also used for visualization and peak integration of .xy files [34]. The Uniprot sequence of human EPO (P01588) without C-terminal arginine was used for the calculations of average masses with the web-based tool ProtPi (<https://www.protpi.ch>). An average mass of 18,235.7324 Da was used for the EPO backbone with 2 disulfide bonds. For glycan building blocks, the residual average masses of hexose (H, 162.1406 Da), *N*-acetylhexosamine (N, 203.19252 Da), deoxyhexose (F, 146.1412 Da), *N*-acetylneuraminic acid (S, 291.2546 Da), *N*-glycolylneuraminic acid (G, 307.2544 Da), acetyl (Ac, 42.0368 Da) and phosphate (P, 79.9799 Da) were used from National Institute of Standards and Technology (<https://www.nist.gov/static/glyco-mass-calc/>). The assignments of glycoform compositions were mainly based on recent data on intact glycoforms, glycopeptides and released glycans of the studied EPO variants [16,27,35]. Analyte curation was based on an  $m/z$  tolerance of 5 Th, a signal-to-noise ratio  $\geq 10$ , and the presence in all replicates. The assigned glycoforms were further validated by simulating the mass spectrum of doubly charged intact EPO ions, using recently published bottom-up data of EPO RS and an R script for simulating mass spectra of intact glycoproteins (<https://github.com/Yang0014/glycoNativeMS>) [16,21]. In addition, the R script was used to assess the similarity of intact EPO RS MALDI mass spectra for the intra- and interday analysis. Relative abundances of intact EPO glycoforms were calculated by total signal intensity normalization. The data were grouped into different glycosylation traits (sialylation, acetylation and LacNAc repeats). For this, all relative intensities were summed based on the number of sialic acids, acetyl groups, or HxN(x-3) repeats. The average number of sialic acids per EPO molecule was determined by summing all relative abundances upon multiplying by the number of sialic acids.

## 3. Results and discussion

### 3.1. Optimization of MALDI MS analysis

The analysis of sialylated glycans and glycoconjugates by MALDI MS may be affected by the loss of sialic acid residues generated from in-source and metastable decay (ISD) processes. The extent of such a loss depends on both the nature of the analyzed biomolecule and the MALDI conditions such as the MALDI matrix and the laser power. Furthermore, the ISD of biomolecules is partially influenced by the pressure of the MALDI ion source [36,37]. It has been shown that the use of an intermediate pressure MALDI ion source minimizes the loss of sialic acid residues of released glycans and glycopeptides [38,39]. Alternatively, sialic acid residues can be stabilized by chemical derivatization as previously shown for the analysis of released glycans and glycopeptides [40–42].

Here, different MALDI matrices, namely CHCA, CICCA, SA, and DHAP, were evaluated for the analysis of EPO RS by MALDI FT-ICR MS (Fig. S2). All matrices allowed for the detection of EPO RS glycoforms. The glycosylation profiles obtained using CICCA and DHAP showed high similarity, whereas the profiles obtained with SA and CHCA showed a significant shift towards less sialylated glycoforms.

This shift, presumably associated with in-source decay processes and consequent loss of sialic acid moieties, was more pronounced for the CHCA matrix. MALDI matrix adducts, detected at high intensity for C1CCA (Fig. S3), were negligible in the mass spectra obtained using DHAP which was chosen for the further analysis of EPO RS by MALDI FT-ICR MS. The use of DHAP, as a “cold” MALDI matrix, and the intermediate pressure MALDI ion source of the FT-ICR MS system minimized sialic acid residue loss of intact EPO RS. The suitability of DHAP for the analysis of sialylated proteins has previously been reported [43].

The obtained mass spectra showed intense doubly charged EPO glycoform signals with intensities ranging over almost two orders of magnitude. The most abundant glycoforms were also detected as singly and triply charged ions but at a lower intensity (Fig. S4). The spectra of the less complex desialylated EPO RS showed a higher abundance of singly charged ions (around 10%) and desialylated EPO RS dimers were detected as doubly and triply charged species (Fig. S4). Due to the low number of observed charge states and their different abundance, the mass spectra were not deconvoluted, instead, the data interpretation and processing was solely based on the doubly charged ions which were measured at a resolving power of about 2,000 (Fig. S5). Of note, MALDI FT-ICR MS has allowed the measurements of small protein and polysaccharides at an isotopic resolution up to about  $m/z$  24,000, providing mass spectra of superior quality compared to MALDI TOF MS [44–56]. Ultrahigh-resolution glycosylation profiles have been obtained for apolipoprotein-CIII, ribonuclease-B, and Fc portions of monoclonal antibodies [50–54]. Isotopic resolution measurements of EPO RS did not improve the mass spectra quality (data not shown) as a consequence of the fast decay of the transient signal that affected the sensitivity of the analysis. EPO RS glycoforms, analyzed by MALDI TOF MS, were not resolved and were instead detected as a single broad peak in line with previous reports (Fig. 2) [29–32,57]. The glycoform resolution in MALDI TOF mass spectra improved after desialylation of the EPO RS, however, also in this case, MALDI FT-ICR MS analysis was more informative.

### 3.2. Glycoform assignments of EPO reference standard

A complex glycosylation profile of EPO RS was obtained by MALDI FT-ICR MS (Fig. 2A, Table S1). Desialylation of EPO RS reduced significantly the mass spectrum complexity and allowed for the assignment of 42 “core” glycoform compositions (Fig. 2B, Table S2). All assignments were based on previously reported glycoform compositions obtained from the characterization of EPO RS samples at the intact protein, the glycopeptide, and the released glycan levels [16,27,35]. Thus, the main “core” glycoforms were assigned to HxN(x-3)F3 compositions generated from the combinatorial occupancy of the four glycosylation sites with varying numbers of antennae and LacNAc (HN) repeats. The largest “core” glycoform was assigned to H30N27F3 while H22N19F3 had the highest abundance. A series of low-abundant HxN(x-5to6)F2P1 “core” glycoforms were also detected. These compositions were associated with phosphorylated (+79.9799 Da) high mannose structures (e.g. H5N2P1, H6N2P1, Fig. S6), which are known to be present at relatively high abundances (summed around 10%) [16]. Of note, HxN(x-6)F2P1, originating from the presence of H6N2P1 at one of the *N*-glycosylation sites, has a compositional difference of  $-2H-1P+2N$  relative to H(x-2)N(x-4)F2 resulting from an unoccupied *N*-glycosylation site which translates into a theoretical  $\Delta m/z$  of  $-1.0620$ . These species could not be resolved and the detected signal was assigned to HxN(x-6)F2P1 glycoforms based on quantitative information on the high mannose glycoforms (i.e. H6N2P1, around 5%) and the occupancy of the *N*-glycosylation sites [16]. In fact, it was previously shown that Asn24 bears the highest levels of

high mannose glycoforms and is the most unoccupied *N*-glycosylation site (around 2%) of the analyzed EPO RS [16]. The assignment of the “core” structures of desialylated EPO RS was further supported by the fact that only phosphorylated high mannose glycoforms were assigned in charge-sensitive high-resolution AEX-MS [16,27]. Although deamidated proteoforms and sulfated (+80.063 Da) glycans of EPO RS were previously reported, these could not be resolved in our analysis [58].

The higher glycoform heterogeneity of the wild-type EPO RS is mainly derived from the presence of a varying number of sialic acids, such as Neu5Ac and to a minor extent Neu5Gc, on the “core” structures (Fig. 2). Additional acetyl groups on the sialic acid residues further increased the complexity. In total, 183 glycoforms were assigned to EPO RS (Table S1, Fig. S7) with the five most abundant glycoforms being H22N19F3S12, H22N19F3S11, H21N18F3S10, H22N19F3S13, H23N20F3S19, in line with previous reports on CHO cell produced EPO [21,27]. On average, for all glycoforms present in a representative replicate, the measurement error was  $-0.5 \pm 1.5$  Th ( $-1.0 \pm 3.0$  Da) based on an external calibration, solely. Mass deviations up to 15.1 Da and 236 glycoforms were instead previously reported for intact EPO glycoforms analyzed by direct native ESI MS analysis [21]. The higher mass tolerance, the potential deconvolution artifacts and the difference in the analyzed EPO samples are possible reasons for the higher number of assigned glycoforms in ESI compared to MALDI.

The possible presence of overlapping signals generated from isobaric glycoforms or glycoforms with similar masses was also evaluated for the assignments. For example, glycoform compositions containing Neu5Gc instead of Neu5Ac differ by 15.995 Da (or  $\Delta m/z$  7.998). This mass difference can also result from the oxidation of Met54 at the protein backbone. However, no detectable amount of oxidized backbone was assigned in the desialylated EPO therefore, this protein modification was excluded. Similarly, both HxN(x-3)F3Sy and H(x+1)N(x-5)F2S(y+1)P1 ( $\Delta m/z$  9.5756) could also be assigned with high confidence. Another example is the compositional difference between 4 HN (+1461.3325 Da) and 5 NeuAc (+1456.2729 Da) that is reflected in a mass difference of 5.0596 Da ( $\Delta m/z$  2.5298). In this case, assignments were based on the mass accuracy, the assigned “core” glycoforms and previous AEX-MS assignments [27]. The assignment of acetylated glycoform compositions also required some additional consideration. Acetylation of sialic acids (up to 2 acetyl groups per sialic acid are possible) of EPO has previously been reported [16,21,27,28,35,59]. Up to 6 acetyl groups were assigned to the most abundant glycoform (H22N19F3S12) of EPO RS (Table S1). Glycoforms with one acetyl group do not overlap with other glycoforms and can be accurately assigned whereas glycoforms with two acetyl groups (HxN(x-3)F3SyAc2) were rarely assigned since glycoforms containing H(x+1)N(x-2)F3S(y-2)G1, with similar masses ( $\Delta m/z$  3.0024), were generally more prominent based on mass accuracy. For compositions with a higher number of acetyl groups, another partial overlap ( $\Delta m/z$  4.9975) between HxN(x-3)F3SyAcz and H(x+1)N(x-2)F3S(y-1)Ac(z-2) was in addition carefully considered for more confident assignments.

Considering the degree of complexity, structural and compositional information obtained using other types of analysis is pivotal to make confident assignments in MALDI FT-ICR mass spectra. In addition to the reported glycosylation analyses of EPO RS, the assignments were further supported by a comparison between the MALDI FT-ICR MS spectra of EPO RS and an *in silico* constructed spectrum obtained from bottom-up glycopeptide data (Table S3) [16], as previously reported by Yang and coworkers [21]. Such a constructed glycosylation profile of EPO RS showed high similarity to the glycoform distribution in the acquired MALDI mass spectrum (Fig. S8) although a shift towards higher sialylation levels was

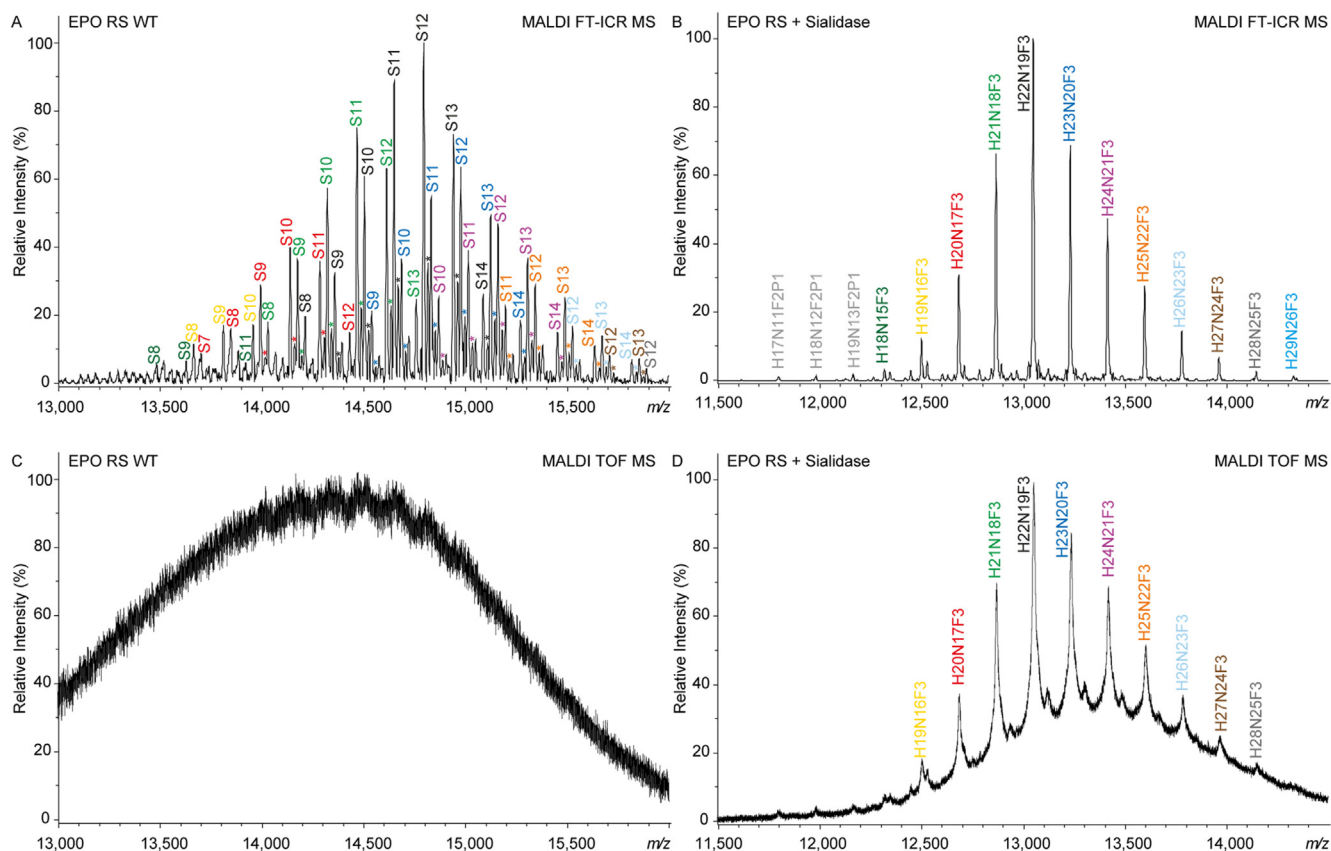


**Fig. 2.** MALDI FT-ICR mass spectra of doubly charged EPO RS (A) wild-type, (B) desialylated and corresponding MALDI TOF mass spectra (C and D, respectively). \* represents acetylated species.

observed in the measured data. This was in line with what was previously shown by Yang and coworkers which compared ESI MS spectra of intact EPO and an *in silico* constructed spectra from glycopeptides data. The observed differences may be explained by the loss of sialic acids and an ionization bias of the sialic acids in bottom-up glycopeptide analysis compared to intact protein characterization. Finally, the glycosylation profiles obtained with MALDI FT-ICR MS were in agreement with previously reported data obtained using bottom-up and intact protein analysis by ESI MS [16,27].

To assess the repeatability of the EPO RS glycosylation profiles obtained by MALDI FT-ICR MS, replicate measurements of EPO RS were performed over three days. The median intra- and inter-day variabilities, calculated for the relative intensities of all glycoform compositions ( $n = 183$ ), were 7.4% and 9.8%, respectively (Table S4). The good repeatability of the EPO glycosylation profiles was corroborated by mass spectra similarity scores higher than 0.96 (Fig. S9).

### 3.3. Glycosylation analysis of EPO variants

Detailed glycosylation profiles of two additional EPO variants, namely EPO RP+ and EPO RP-, were obtained using the MALDI FT-ICR MS method optimized for the analysis of EPO RS (Fig. 3, Tables S5 and S6). These variants were recently characterized by QC release methods, bottom-up LC-MS and AEX-MS at the intact level [5,16,27]. In the MALDI FT-ICR MS spectra, 169 and 199 glycoform compositions were assigned to EPO RP+ and EPO RP-, respectively, whereas 160 and 192 glycovariants (deamidated proteoforms not included) were previously assigned by AEX-MS. A higher number of

LacNAc repeats was detected by MALDI FT-ICR MS for EPO RP+ compared to EPO RS, in line with bottom-up LC-MS data (mainly at Asn83) [5]. The MALDI spectra of EPO RP- indicated lower levels of *N*-glycosylation. Instead, glycoforms with only two occupied *N*-glycosylation sites (HxNx-2F2Sy) were assigned for EPO RP-, e.g. the most abundant species was assigned to H15N13F2S9 instead of H17N11F2S9P1 (assigned glycoform for EPO RS), in line with the previously reported low site occupancy of Asn24 [5].

Key glycosylation features of the three different EPO variants were compared (Fig. 4). The average number of sialic acids, determined by MALDI FT-ICR MS, was 10.7 (EPO RS), 10.9 (EPO RP+) and 9.4 (EPO RP-). This is in good agreement with QC release, bottom-up LC-MS and AEX-MS analyses previously reported for the same EPO variants (Table 1). MALDI FT-ICR MS showed the same sialylation ranking (EPO RP+ > EPO RS > EPO RP-), except for the AEX-MS method (EPO RS > EPO RP+ > EPO RP-). Considering the QC release method as the best estimation of sialylation, the sialic acid stability of the MALDI FT-ICR MS method is above 95%.

Other glycosylation quality features such as LacNAc repeats and acetylation can also be derived from the MALDI FT-ICR mass spectra (Fig. 4). In line with previous reports, 70%–80% of the sialic acids are not acetylated [27]. Mono-acetylated species were below 20% and higher degrees of acetylated glycoforms should be carefully interpreted owing to described overlapping species. The expected differences in the LacNAc repeats of the different EPO variants could be shown as well by the relative quantification (Fig. 4). The distribution of HxN(x-3)F3 species obtained for EPO RS was in good agreement with the analysis upon desialylation (Fig. 2). EPO RP+ showed the highest content of HN units (H24N21F3 most

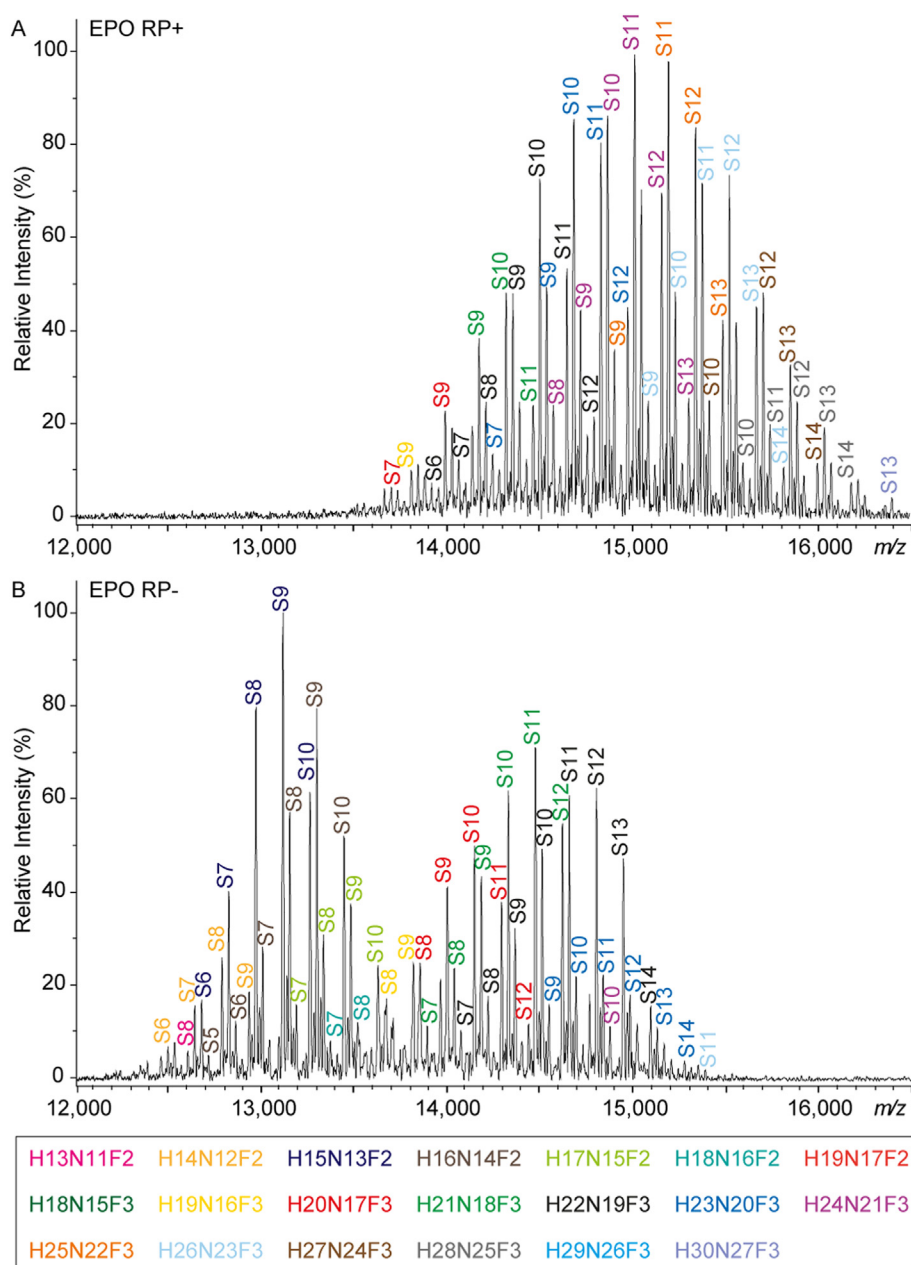


Fig. 3. MALDI FT-ICR mass spectra of EPO variants with (A) increased number of LacNAc units and (B) decreased glycosylation site occupancy.

abundant) and both EPO RS and EPO RP- showed H22N19F3 as the most abundant species.

It should be stressed that prior knowledge of glycosylation moieties of complex glycoproteins, such as EPO, is needed for a reliable interpretation of intact protein mass spectra. Such information must be obtained by a multi-level structural characterization of the glycoproteins which includes released glycan analysis and site-specific characterization by bottom-up MS. Nonetheless, as depicted in Fig. 1, a comprehensive characterization of EPO must include the analysis at the intact protein level to determine the combinatory presence of protein modifications on different modification sites. This unique information is key for assessing the structural integrity, quality, and safety of pharmaceutical proteins.

#### 4. Conclusions

In this study, we showed that detailed glycosylation profiles of intact EPO can be obtained by low-resolution MALDI FT-ICR MS. An exceptional improvement in glycoform resolution was achieved compared to MALDI TOF MS analysis. MALDI FT-ICR MS provided glycosylation profiles comparable to data previously obtained with other types of analyses such as native ESI MS and AEX-MS and allowed for a more straightforward data acquisition and interpretation. In fact, MALDI FT-ICR MS allowed for the measurements of multiple samples without the need for in-between washing steps as for native ESI MS, while the evaluation of only doubly charged ions made deconvolution unnecessary. The comparison of the glycosylation profiles of three different EPO variants, namely EPO

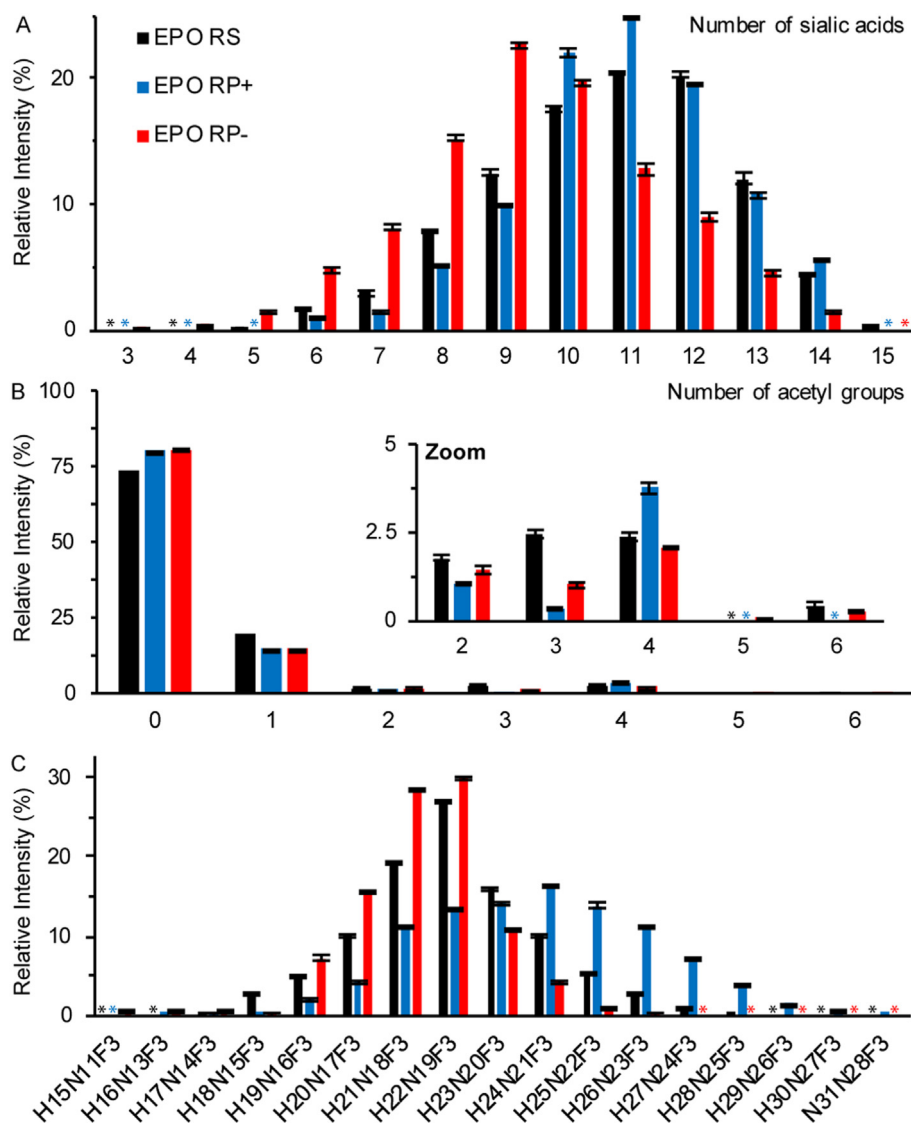


Fig. 4. Key glycosylation features of three EPO variants analyzed by MALDI FT-ICR MS. (A) Sialylation, (B) acetylation and (C) LacNAc repeats. \* not detected.

Table 1

Comparison of the average sialic acid content per EPO molecule determined by different methods.

Method	EPO RS	EPO RP+	EPO RP-
<b>MALDI FT-ICR MS</b>	<b>10.7 ± 0.03</b>	<b>10.9 ± 0.01</b>	<b>9.4 ± 0.04</b>
QC [5] <sup>a</sup>	11.2 ± 0.05	11.4 <sup>c</sup>	10.2 <sup>c</sup>
MAM [5] <sup>b</sup>	10.9 ± 0.1	10.4 <sup>c</sup>	10.1 <sup>c</sup>
AEX-MS [27]	11.6 ± 0.04	11.4 ± 0.08	11.0 ± 0.13

<sup>a</sup> HPAEC-PAD analysis of released sialic acids (Neu5Ac).

<sup>b</sup> Multiple Attribute Monitoring by bottom-up LC-MS of a GluC digest.

<sup>c</sup> Standard deviations not available.

RS, EPO RP+ and EPO RP-, showed that MALDI FT-ICR MS allows for the evaluation of key glycosylation features such as the number of sialic acid residues and acetyl groups and LacNAc repeats. In particular, sialylation – the most important and susceptible glycosylation trait of EPO – was proven to be stable under the chosen MALDI conditions and sialylation profiles were in good agreement with those obtained from other orthogonal methods. Of note, as the loss of sialic acid during MALDI also depends on the nature of the analyzed biomolecule, different spotting conditions

and/or acquisition parameters may be required for the analysis of different glycoproteins. Finally, the simplicity and potential high-throughput capability of the here developed method are desirable characteristics for applications in the biopharmaceutical industry. Further studies are needed to evaluate the applicability of the developed method for the analysis of unpurified EPO during the manufacturing process and to evaluate (and develop) more accessible MS technology (e.g. MALDI qTOF MS) that could provide similar mass spectral quality of EPO glycoforms as obtained using 15T MALDI FT-ICR MS. To our knowledge, this is the first report on the use of MALDI MS for the glycoform-resolved analysis of highly sialylated intact glycoproteins. We anticipate the application of our strategy for the analysis of different pharmaceutical glycoproteins with a molecular mass of up to 40 kDa including various hormones and glycoconjugate vaccines.

#### CRedit authorship contribution statement

**Steffen Lippold:** designed the experiments, performed the measurements, evaluated the data, drafted the manuscript. **Raashina Thavarajah:** performed initial tests. **Dietmar Reusch:**



designed the experiments. **Manfred Wuhrer**: designed the experiments. **Simone Nicolardi**: designed the experiments, performed the measurements, drafted the manuscript. The manuscript was finalized through the contributions of all authors. All authors have approved the final version.

### Declaration of competing interest

The authors declare the following financial interests/personal relationships which may be considered as potential competing interests: Dietmar Reusch is an employee of Roche Diagnostics GmbH. All other authors declare no conflict of interest.

### Acknowledgments

This research was funded by the European Union (European Commission H2020, Analytics for Biologics project, Grant 765502).

### Appendix A. Supplementary data

Supplementary data to this article can be found online at <https://doi.org/10.1016/j.aca.2021.339084>.

### References

- [1] C. Winearls, M. Pippard, M. Downing, D. Oliver, C. Reid, P. Mary Cotes, Effect of human erythropoietin derived from recombinant DNA on the anaemia of patients maintained by chronic haemodialysis, *Lancet* 328 (1986) 1175–1178.
- [2] W. Jelkmann, Erythropoietin: structure, control of production, and function, *Physiol. Rev.* 72 (1992) 449–489.
- [3] T.B. Drüeke, F. Locatelli, N. Clyne, K.-U. Eckardt, I.C. Macdougall, D. Tsakiris, H.-U. Burger, A. Scherhag, C. Investigators, Normalization of hemoglobin level in patients with chronic kidney disease and anemia, *N. Engl. J. Med.* 355 (2006) 2071–2084.
- [4] M. Nimtz, W. Martin, V. Wray, K.-D. Klöppel, J. Augustin, H.S. Conrath, Structures of sialylated oligosaccharides of human erythropoietin expressed in recombinant BHK-21 cells, *Eur. J. Biochem.* 213 (1993) 39–56.
- [5] A. Buettner, M. Maier, L. Bonnington, P. Bulau, D. Reusch, Multi-attribute monitoring of complex erythropoietin beta glycosylation by GluC liquid chromatography–mass spectrometry peptide mapping, *Anal. Chem.* 92 (2020) 7574–7580.
- [6] W.R. Alley, B.F. Mann, M.V. Novotny, High-sensitivity analytical approaches for the structural characterization of glycoproteins, *Chem. Rev.* 113 (2013) 2668–2732.
- [7] M. Girard, A. Puerta, J.C. Diez-Masa, M. de Frutos, High resolution separation methods for the determination of intact human erythropoiesis stimulating agents, A review, *Anal. Chim. Acta* 713 (2012) 7–22.
- [8] E. Balaguer, C. Neusüss, Glycoprotein characterization combining intact protein and glycan analysis by capillary electrophoresis–electrospray ionization–mass spectrometry, *Anal. Chem.* 78 (2006) 5384–5393.
- [9] R.G. Jayo, M. Thaysen-Andersen, P.W. Lindenburg, R. Haselberg, T. Hankemeier, R. Ramautar, D.D.Y. Chen, Simple capillary electrophoresis–mass spectrometry method for complex glycan analysis using a flow-through microvial interface, *Anal. Chem.* 86 (2014) 6479–6486.
- [10] A. Shubhakar, R.P. Kozak, K.R. Reiding, L. Royle, D.I.R. Spencer, D.L. Fernandes, M. Wuhrer, Automated high-throughput permethylation for glycosylation analysis of Biologics using MALDI-TOF-MS, *Anal. Chem.* 88 (2016) 8562–8569.
- [11] P. Capdeville, L. Martin, S. Cholet, A. Damont, M. Audran, M. Ericsson, F. Fenaille, A. Marchand, Evaluation of erythropoietin biosimilars Epotin™, Hemax® and Jimaixin™ by electrophoretic methods used for doping control analysis and specific N-glycan analysis revealed structural differences from original epoetin alfa drug Eprex®, *J. Pharmaceut. Biomed. Anal.* 194 (2021) 113750.
- [12] H. Sasaki, N. Ochi, A. Dell, M. Fukuda, Site-specific glycosylation of human recombinant erythropoietin: analysis of glycopeptides or peptides at each glycosylation site by fast atom bombardment–mass spectrometry, *Biochemistry* 27 (1988) 8618–8626.
- [13] R.S. Rush, P.L. Derby, D.M. Smith, C. Merry, G. Rogers, M.F. Rohde, V. Katta, Microheterogeneity of erythropoietin carbohydrate structure, *Anal. Chem.* 67 (1995) 1442–1452.
- [14] N. Kawasaki, M. Ohta, S. Hyuga, M. Hyuga, T. Hayakawa, Application of liquid chromatography/mass spectrometry and liquid chromatography with tandem mass spectrometry to the analysis of the site-specific carbohydrate heterogeneity in erythropoietin, *Anal. Biochem.* 285 (2000) 82–91.
- [15] D. Kolarich, P.H. Jensen, F. Altmann, N.H. Packer, Determination of site-specific glycan heterogeneity on glycoproteins, *Nat. Protoc.* 7 (2012) 1285–1298.
- [16] S. Lippold, A. Büttner, M.S.F. Choo, M. Hook, C.J. de Jong, T. Nguyen-Khuong, M. Habberger, D. Reusch, M. Wuhrer, N. de Haan, Cysteine aminoethylation enables the site-specific glycosylation analysis of recombinant human erythropoietin using trypsin, *Anal. Chem.* 92 (2020) 9476–9481.
- [17] E. Giménez, R. Ramos-Hernan, F. Benavente, J. Barbosa, V. Sanz-Nebot, Analysis of recombinant human erythropoietin glycopeptides by capillary electrophoresis electrospray–time of flight–mass spectrometry, *Anal. Chim. Acta* 709 (2012) 81–90.
- [18] E. Watson, A. Bhide, H. van Halbeek, Structure determination of the intact major sialylated oligosaccharide chains of recombinant human erythropoietin expressed in Chinese hamster ovary cells, *Glycobiology* 4 (1994) 227–237.
- [19] C. Neusüss, U. Demelbauer, M. Pelzing, Glycoform characterization of intact erythropoietin by capillary electrophoresis–electrospray–time of flight–mass spectrometry, *Electrophoresis* 26 (2005) 1442–1450.
- [20] E. Giménez, F. Benavente, J. Barbosa, V. Sanz-Nebot, Analysis of intact erythropoietin and novel erythropoiesis-stimulating protein by capillary electrophoresis–electrospray–ion trap mass spectrometry, *Electrophoresis* 29 (2008) 2161–2170.
- [21] Y. Yang, F. Liu, V. Franc, L.A. Halim, H. Schellekens, A.J.R. Heck, Hybrid mass spectrometry approaches in glycoprotein analysis and their usage in scoring biosimilarity, *Nat. Commun.* 7 (2016) 13397.
- [22] A. Pantazaki, M. Taverna, C. Vidal-Madjar, Recent advances in the capillary electrophoresis of recombinant glycoproteins, *Anal. Chim. Acta* 383 (1999) 137–156.
- [23] E. Domínguez-Vega, S. Tengattini, C. Peintner, J. van Angeren, C. Temporini, R. Haselberg, G. Massolini, G.W. Somsen, High-resolution glycoform profiling of intact therapeutic proteins by hydrophilic interaction chromatography–mass spectrometry, *Talanta* 184 (2018) 375–381.
- [24] A. Harazono, N. Hashii, R. Kuribayashi, S. Nakazawa, N. Kawasaki, Mass spectrometric glycoform profiling of the innovator and biosimilar erythropoietin and darbepoetin by LC/ESI-MS, *J. Pharmaceut. Biomed. Anal.* 83 (2013) 65–74.
- [25] R. Haselberg, G.J. de Jong, G.W. Somsen, Low-flow sheathless capillary electrophoresis–mass spectrometry for sensitive glycoform profiling of intact pharmaceutical proteins, *Anal. Chem.* 85 (2013) 2289–2296.
- [26] A. Taichrib, M. Pelzing, C. Pellegrino, M. Rossi, C. Neusüss, High resolution TOF MS coupled to CE for the analysis of isotopically resolved intact proteins, *J. Proteom.* 74 (2011) 958–966.
- [27] G. van Schaick, C. Gstöttner, A. Büttner, D. Reusch, M. Wuhrer, E. Domínguez-Vega, Anion exchange chromatography – mass spectrometry for monitoring multiple quality attributes of erythropoietin biopharmaceuticals, *Anal. Chim. Acta* 1143 (2021) 166–172.
- [28] T. Caval, W. Tian, Z. Yang, H. Clausen, A.J.R. Heck, Direct quality control of glycoengineered erythropoietin variants, *Nat. Commun.* 9 (2018) 3342.
- [29] S.M.R. Stanley, A. Poljak, Matrix-assisted laser-desorption time-of flight ionisation and high-performance liquid chromatography–electrospray ionisation mass spectral analyses of two glycosylated recombinant epoetins, *J. Chromatogr. B* 785 (2003) 205–218.
- [30] E. Giménez, F. Benavente, J. Barbosa, V. Sanz-Nebot, Towards a reliable molecular mass determination of intact glycoproteins by matrix-assisted laser desorption/ionization time-of-flight mass spectrometry, *Rapid Commun. Mass Spectrom.* 21 (2007) 2555–2563.
- [31] E. Llop, R. Gutiérrez-Gallego, J. Segura, J. Mallorquí, J.A. Pascual, Structural analysis of the glycosylation of gene-activated erythropoietin (epoetin delta, Dynepo), *Anal. Biochem.* 383 (2008) 243–254.
- [32] E. Giménez, F. Benavente, J. Barbosa, V. Sanz-Nebot, Ionic liquid matrices for MALDI-TOF-MS analysis of intact glycoproteins, *Anal. Bioanal. Chem.* 398 (2010) 357–365.
- [33] X. Lou, J.L.J. van Dongen, E.W. Meijer, Generation of CsI cluster ions for mass calibration in matrix-assisted laser desorption/ionization mass spectrometry, *J. Am. Soc. Mass Spectrom.* 21 (2010) 1223–1226.
- [34] M. Strohal, M. Hassman, B. Kořata, M. Kofíček, mMass data miner: an open source alternative for mass spectrometric data analysis, *Rapid Commun. Mass Spectrom.* 22 (2008) 905–908.
- [35] D. Falck, M. Habberger, R. Plomp, M. Hook, P. Bulau, M. Wuhrer, D. Reusch, Affinity purification of erythropoietin from cell culture supernatant combined with MALDI-TOF-MS analysis of erythropoietin N-glycosylation, *Sci. Rep.* 7 (2017) 5324.
- [36] J. Soltwisch, J. Souady, S. Berkenkamp, K. Dreisewerd, Effect of gas pressure and gas type on the fragmentation of peptide and oligosaccharide ions generated in an elevated pressure UV/IR-MALDI ion source coupled to an orthogonal time-of-flight mass spectrometer, *Anal. Chem.* 81 (2009) 2921–2934.
- [37] D. Asakawa, D. Calligaris, T.A. Zimmerman, E. De Pauw, In-source decay during matrix-assisted laser desorption/ionization combined with the collisional process in an FTICR mass spectrometer, *Anal. Chem.* 85 (2013) 7809–7817.
- [38] M.H.J. Selman, L.A. McDonnell, M. Palmblad, L.R. Ruhaak, A.M. Deelder, M. Wuhrer, Immunoglobulin G glycopeptide profiling by matrix-assisted laser desorption/ionization fourier transform ion cyclotron resonance mass spectrometry, *Anal. Chem.* 82 (2010) 1073–1081.
- [39] K.R. Reiding, L.R. Ruhaak, H.-W. Uh, S. el Bouhaddani, E.B. van den Akker, R. Plomp, L.A. McDonnell, J.J. Houwing-Duistermaat, P.E. Slagboom, M. Beekman, M. Wuhrer, Human plasma N-glycosylation as analyzed by matrix-assisted laser desorption/ionization–fourier transform ion cyclotron resonance-MS associates with markers of inflammation and metabolic health, *Mol. Cell. Proteomics* 16 (2017) 228–242.

- [40] N. de Haan, S. Yang, J. Cipollo, M. Wührer, Glycomics studies using sialic acid derivatization and mass spectrometry, *Nat. Rev. Chem.* 4 (2020) 229–242.
- [41] N. de Haan, K.R. Reiding, M. Habberger, D. Reusch, D. Falck, M. Wührer, Linkage-specific sialic acid derivatization for MALDI-TOF-MS profiling of IgG glycopeptides, *Anal. Chem.* 87 (2015) 8284–8291.
- [42] H. Li, W. Gao, X. Feng, B.-F. Liu, X. Liu, MALDI-MS analysis of sialylated N-glycan linkage isomers using solid-phase two step derivatization method, *Anal. Chim. Acta* 924 (2016) 77–85.
- [43] J.J. Pitt, J.J. Gorman, Matrix-assisted laser desorption/ionization time-of-flight mass spectrometry of sialylated glycopeptides and proteins using 2,6, Dihydroxyacetophenone as a Matrix 10 (1996) 1786–1788.
- [44] J.A. Castoro, C.L. Wilkins, Ultrahigh resolution matrix-assisted laser desorption/ionization of small proteins by Fourier-transform mass spectrometry, *Anal. Chem.* 65 (1993) 2621–2627.
- [45] M.L. Easterling, C.C. Pitsenberger, S.S. Kulkarni, P.K. Taylor, I.J. Amster, A 4.7 Tesla internal MALDI-FTICR instrument for high mass studies: performance and methods, *Int. J. Mass Spectrom. Ion Process.* 157–158 (1996) 97–113.
- [46] A.G. Marshall, C.L. Hendrickson, G.S. Jackson, Fourier transform ion cyclotron resonance mass spectrometry: a primer, *Mass Spectrom. Rev.* 17 (1998) 1–35.
- [47] H.-Q. Nguyen, D. Lee, Y. Kim, M. Paek, M. Kim, K.-S. Jang, J. Oh, Y.-S. Lee, J.E. Yeon, D.M. Lubman, J. Kim, Platelet factor 4 as a novel exosome marker in MALDI-MS analysis of exosomes from human serum, *Anal. Chem.* 91 (2019) 13297–13305.
- [48] F. Fleurbaaij, M.E.M. Kraakman, E.C.J. Claas, C.W. Knetusch, H.C. van Leeuwen, Y.E.M. van der Burgt, K.E. Veldkamp, M.C. Vos, W. Goessens, B.J. Mertens, E.J. Kuijper, P.J. Hensbergen, S. Nicolardi, Typing *Pseudomonas aeruginosa* isolates with ultrahigh resolution MALDI-FTICR mass spectrometry, *Anal. Chem.* 88 (2016) 5996–6003.
- [49] J.M. Spraggins, D.G. Rizzo, J.L. Moore, M.J. Noto, E.P. Skaar, R.M. Caprioli, Next-generation technologies for spatial proteomics: integrating ultra-high speed MALDI-TOF and high mass resolution MALDI FTICR imaging mass spectrometry for protein analysis, *Proteomics* 16 (2016) 1678–1689.
- [50] B.M. Prentice, D.J. Ryan, R. Van de Plas, R.M. Caprioli, J.M. Spraggins, Enhanced ion transmission efficiency up to  $m/z$  24 000 for MALDI protein imaging mass spectrometry, *Anal. Chem.* 90 (2018) 5090–5099.
- [51] S. Nicolardi, L. Switzar, A.M. Deelder, M. Palmblad, Y.E.M. van der Burgt, Top-down MALDI-in-source decay-FTICR mass spectrometry of isotopically resolved proteins, *Anal. Chem.* 87 (2015) 3429–3437.
- [52] S. Nicolardi, Y.E.M. van der Burgt, M. Wührer, A.M. Deelder, Mapping O-glycosylation of apolipoprotein C-III in MALDI-FT-ICR protein profiles, *Proteomics* 13 (2013) 992–1001.
- [53] Y.E.M. van der Burgt, D.P.A. Kilgour, Y.O. Tsybin, K. Szrentic, L. Fornelli, A. Beck, M. Wührer, S. Nicolardi, Structural analysis of monoclonal antibodies by ultrahigh resolution MALDI in-source decay FT-ICR mass spectrometry, *Anal. Chem.* 91 (2019) 2079–2085.
- [54] C. Gstottner, D. Reusch, M. Habberger, I. Dragan, P. Van Veelen, D.P.A. Kilgour, Y.O. Tsybin, Y.E.M. van der Burgt, M. Wührer, S. Nicolardi, Monitoring glycation levels of a bispecific monoclonal antibody at subunit level by ultrahigh-resolution MALDI FT-ICR mass spectrometry, *mAbs* 12 (2020) 1682403.
- [55] S. Nicolardi, A.A. Joseph, Q. Zhu, Z. Shen, A. Pardo-Vargas, F. Chiodo, A. Molinaro, A. Silipo, Y.E.M. van der Burgt, B. Yu, P.H. Seeberger, M. Wührer, Analysis of synthetic monodisperse polysaccharides by wide mass range ultrahigh-resolution MALDI mass spectrometry, *Anal. Chem.* 93 (10) (2021) 4666–4675.
- [56] Q. Zhu, Z. Shen, F. Chiodo, S. Nicolardi, A. Molinaro, A. Silipo, B. Yu, Chemical synthesis of glycans up to a 128-mer relevant to the O-antigen of *Bacteroides vulgatus*, *Nat. Commun.* 11 (2020) 4142.
- [57] G. Stübiger, M. Marchetti, M. Nagano, C. Reichel, G. Gmeiner, G. Allmaier, Characterisation of intact recombinant human erythropoietins applied in doping by means of planar gel electrophoretic techniques and matrix-assisted laser desorption/ionisation linear time-of-flight mass spectrometry 19 (2005) 728–742.
- [58] Z. Szabo, J.R. Thayer, D. Reusch, Y. Agroskin, R. Viner, J. Rohrer, S.P. Patil, M. Krawitzky, A. Huhmer, N. Avdalovic, S.H. Khan, Y. Liu, C. Pohl, High performance anion exchange and hydrophilic interaction liquid chromatography approaches for comprehensive mass spectrometry-based characterization of the N-glycome of a recombinant human erythropoietin, *J. Proteome Res.* 17 (2018) 1559–1574.
- [59] S. Hua, M.J. Oh, S. Ozcan, Y.S. Seo, R. Grimm, H.J. An, Technologies for glycomic characterization of biopharmaceutical erythropoietins, *Trends Anal. Chem.* 68 (2015) 18–27.